Synthesis and Characterization of Janus Gold Nanoparticles

*Hyewon Kim, Randy P. Carney, Javier Reguera, Quy K. Ong, Xiang Liu, and Francesco Stellacci**

Ligand molecules on monolayer-protected gold nanoparticles (NPs) determine the majority of their surface properties. It has been established that when a binary mixture of dislike ligands forms a self-assembled monolayer either on flat surfaces[1] or on a NP,[2] separation into distinct domains occurs. For gold NPs between ~3 and ~8 nm in diameter, stripe-like domains form.[2b,3] This happens because of a balance between the enthalpy of phase separation and the interfacial entropy that arises due to a size/length mismatch between two ligand molecules.[3,4] It has been predicted that as NPs become smaller, the interfacial entropy contribution becomes less and less relevant, since the increase in the cone angle that delimits the ligands yields an overall increase in conformational entropy for the entire chain (**Figure 1**). Under this condition, the final morphology is primarily determined by the enthalpy of separation; hence, for small particles, the spontaneous formation of completely separated distributions of ligands, i.e., the formation of Janus particles, has been predicted.[4] Here, we report that gold NPs with a core diameter smaller than ~1.5 nm form Janus NPs in many ligand combinations. We synthesized four different types of gold NPs with varying ligand combinations and characterized them using 2D NMR, analytical ultracentrifugation (AUC), gel electrophoresis (GEP), and scanning tunneling microscopy (STM). All of these techniques confirm the presence of a majority of Janus particles and show similar cutoff sizes for the Janus-to-stripe transition.

Ligand shell-protected NPs have drawn interest as new building blocks in chemistry; they have a central core, whose size and shape can be readily changed, and a coating that can be composed of multiple patches varying in chemical affinity.[5] Patchiness in the ligand shell coating can impart key properties to the particles.[5,6] Patchy particles have potential applications that range from photonic crystals[7] to drug delivery.[8] Many theoretical studies have investigated their physical properties,[6,9] and various approaches exist to fabricate patchy particles.[10] Janus particles, defined as biphasic particles, are a particularly important class of patchy particles.[11] They have been studied not only for industrial application such as e-ink displays,[12] catalysis,[13] anti-reflective coatings,[14] and emulsifying agents,[15] but also for fundamental studies that establish their assembly properties as well as their use as surfactant particles.[16] Several synthetic methods for the fabrication of Janus particles currently exist. Examples include microfluidics,[17] biphasic electrohydrodynamic jetting,[18] layer-by-layer assembly,[19] and stepwise functionalization of immobilized particles.[20] In this paper, we introduce a new method to synthesize Janus monolayer-protected gold NPs. This is an easy, scalable, one-step, and single-pot method used to produce the smallest kind of Janus particles to date.

When two dislike thiolated molecules are self-assembled on gold NPs, as well as on flat gold surfaces,[1] they separate into distinct domains due to their immiscibility.[4] Our group has shown that stripe-like domains form on gold NPs when they are coated with a self-assembled monolayer composed of a binary mixture of dissimilar ligands. This was done using scanning tunneling microscopy (STM),[2b] infrared (IR) spectroscopy,[21] and more recently nuclear magnetic resonance (NMR).[22] It was established that striped NPs exhibit a set of properties that derive directly from the morphology of their ligand shell.[2b,21,23] For example, they show a non-monotonic dependence of their solubility[21] and interfacial energy[23a] on their ligand shell composition, implying a strong effect of the striped morphology on these properties. Similar results have been found in molecular recognition[23e] and catalysis.[23d] Additionally, striped NPs have two distinct regions at polar opposites where the stripes 'collapse' into point defects. These polar point defects are more thermodynamically active and can be chemically modified into divalent NPs that can be reacted to form chains.[23c] Moreover, these chains form only for NPs of ~3 nm to ~ 8 nm in diameter implying that the striped morphology would form only on NPs of those sizes.[3]

Stripe-like morphology, and more generally small patchy domains, form on the NPs due to competition between the enthalpy of phase-separation and the conformational entropy that arises at the interface between longer and shorter ligands (Figure 1a).[4] The enthalpy of a self-assembled monolayer composed of dissimilar ligands will be minimized when the number of similar ligands packed together is maximized. We can say that such a system will tend to minimize the length of the interfacial line. Therefore, enthalpically, striped NPs are not favored. However, the conformational entropy of each long ligand molecule will increase if it is surrounded by shorter ligands, since there will be additional free volume around 'extra lengths' of the longer ligands (Figure 1a). The balance between the enthalpy of phase-separation and this conformational entropy determines the formation of striped NPs, as shown by coarse-grained and molecular dynamics simulations.[4] However, these simulations

R. P. Carney, Dr. J. Reguera, Dr. Q. K. Ong, Dr. X. Liu, Prof. F. Stellacci
Institute of Materials
École Polytechnique Fédérale de Lausanne
EPFL-STI-IMX-SuNMIL, Lausanne CH-1015, Switzerland
E-mail: francesco.stellacci@epfl.ch

H. Kim
Department of Materials Science and Engineering
Massachusetts Institute of Technology
77 Massachusetts Ave., Cambridge, MA 02139, USA

DOI: 10.1002/adma.201200926

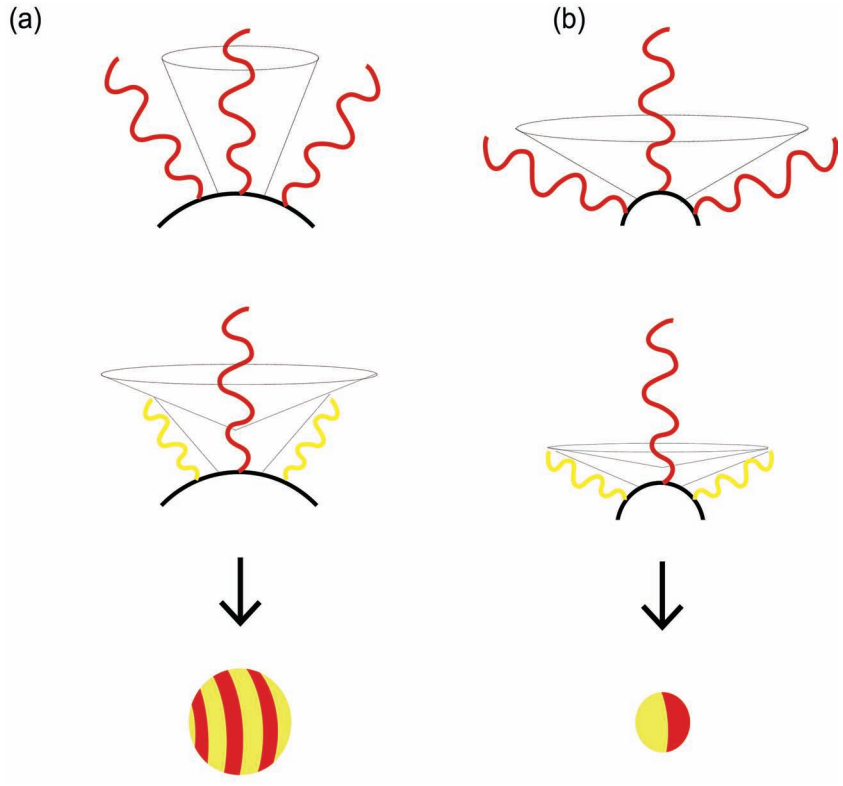

Figure 1. Schematic drawing illustrating the conformational entropy for ligands on NPs. On the top there are cartoons of ligands on NPs, on the bottom the predicted nanoparticle morphology. For relatively larger radii of curvature (a) the presence of shorter ligands allows longer ones to have a larger free volume; and hence, gain conformational entropy. One can divide the cone that shows a free volume of a long ligand in two parts: one whose angle is determined by the packing of the molecules and the other due to this interfacial free volume. (b) As the radius of curvature decreases, the first cone becomes the dominant, and make the second one irrelevant.

as well as experiments show that striped NPs only exist in a certain size range.[3,4] Simulations predict that in smaller NPs, Janus arrangement will spontaneously form; that is, the ligands separate into two bulk phases. This is because the smaller radius of curvature provides each ligand with a larger overall free volume, making the extra-length interfacial configurational entropy mostly irrelevant (Figure 1b). The existence of Janus NPs has been predicted by simulation, but it has hitherto not been confirmed by experiment.

To determine whether small bi-ligand gold particles have Janus morphology, we synthesized four different types of gold NPs with four ligand combinations. NPs with small core diameters were synthesized using the one-phase method[24] and a modified Stucky method.[25] For the one-phase method, we have found that nanoparticle synthesis at low temperature results in particles of small sizes. We used the one-phase method in ethanol[24] at 0 °C for synthesizing gold NPs covered with 3-mercapto-1-propanesulfonate (MPSA) and *N,N,N*-trimethyl(11-mercaptoundecyl) ammonium bromide (TMA). We used a modified Stucky method[25] for synthesizing three different gold NPs. The first NPs were covered with hexadecane-1-thiol (HDT) and 1,1′,4′,1″-terphenyl-4-thiol (TPT) in dichloromethane at 0 °C. The second NPs were covered with tetradecane-1-thiol (TDT) and 11-amino-1-undecanethiol (AUDT) in 1:2 mixture of chloroform and methanol at 60 °C. The last NPs were covered with 11-mercaptoundecanoic acid (MUA) and 1-octanethiol (OT) in 1:1 mixture of toluene and methanol at 100 °C. For this modified Stucky synthesis, we controlled the size mostly through the gold to ligand ratio and the choice of the solvent as well as temperature. The sizes of all NPs were characterized using transmission electron microscopy (TEM) with ImageJ software and the analysis of at least 200 particles. Hereafter, we refer to NP composition as the stoichiometric ratio used in the reaction. We know that the real ligand shell composition[22] differs from the actual one, but this difference is not relevant for the arguments in this paper.

First, we investigated the morphology of HDT and TPT coated NPs using nuclear Overhauser enhancement spectroscopy (NOESY). A recent study by Pradhan et al. showed that NOESY can be used to determine Janus morphology on NPs' ligand shell, because when this morphology is present, cross-peaks between the hydrogen on one type of ligand molecules and the hydrogen on the other type nearly disappear.[26] Recent work in our group by Liu et al. has confirmed this approach.[22] In order to use NOESY, we chose HDT and TPT, since their ^{1}H chemical shifts do not overlap with each other. Since NOESY shows cross-peaks only for short-range dipole-dipole interactions between nuclear spins, the cross-peaks between HDT and TPT would exist only when two molecules are close together. In the case of Janus NPs, there should be a very weak cross-peak or no cross-peak because only a relatively small interface between two ligands exists. To perform our study, we chose a comparative approach synthesizing particles of different sizes (the core diameters of ~2.0 nm and ~4.5 nm) with identical ligand shell composition. The NOESY spectra of these two NPs covered with HDT/TPT are shown in **Figure 2**. The NOESY NMR spectrum of small gold NPs (~2.0 nm) shows no cross-peaks between HDT and TPT (Figure 2a). In clear contrast, obvious cross-peaks are observed with the larger size (~ 4.5 nm) NPs (Figure 2b). This result confirms that gold NPs with small cores form Janus NPs.

Janus structure can also be confirmed by chemically linking gold NPs. To achieve this goal, NPs coated with a 2:1 ratio of TDT/AUDT were prepared, so that the amine group at the end of AUDT would react with sebacoyl chloride (SC), leading to dimers of NPs. Our hypothesis is that Janus particles will form mostly dimers in the right reaction conditions, while dimers would be an unlike reaction product for most other morphologies. This is because once a dimer is formed, there would be significant steric hindrance preventing the third particle from reacting with the core of the dimer assembly. TDT/AUDT NPs were reacted with SC in dichloromethane for 10 min, and were

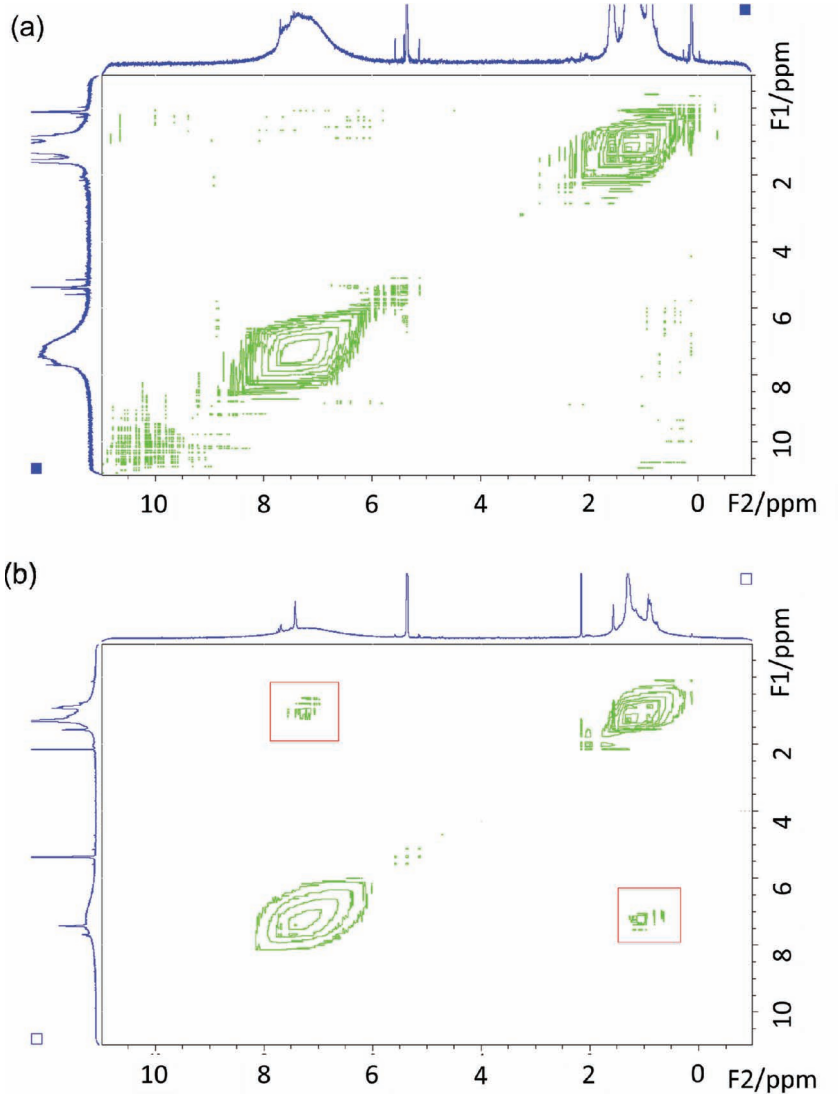

Figure 2. NOESY measurements of HDT/TPT mixed ligand coated NPs. (a) NOESY measurement of Janus NPs; (b) NOESY measurement of striped NPs with the same ligand composition. Clear cross-peaks shown in striped NPs (red box) disappear in small NPs, which indicate two ligands phase-separate as Janus NPs. The sharp peaks observed in the spectra are solvent peak (~5.3 ppm dichloromethane, ~2.1 ppm acetone).

filtered using Sephadex column. NPs were separated into two populations during filtration. Both the fraction that moved through the column and the fraction that did not were characterized using TEM (**Figure 3**). Dimers could be found only in the latter, indicating that these aggregates were covalently bonded during the reactions and were not a dynamic assembly product. We analyzed TEM images to determine the size of particles that formed dimers. As shown in Figure 3c, only NPs smaller than 3 nm formed dimers. Also, the average diameter of NPs forming dimers was 1.8 ± 0.4 nm. In addition to TEM analysis, we performed analytical ultracentrifugation (AUC), a technique allowing the detection of dimers in solution. AUC measures sedimentation properties of materials that depend on size, shape, and density of the material. It is widely used in biology to separate and characterize proteins in their mass and structure. Recently, our group used AUC to determine the size, density, and molecular weight of gold NPs dispersed in solution.[27] AUC experiments were performed before and after dimerization, and the change in size and shape distribution of NPs was measured. AUC data were first used to confirm the size of the particles determined by TEM (Figure 3d). We then used AUC to analyze the effect of the dimerization reaction. As evident from the comparison of figure 3c and 3d, a sizeable part of the fraction of particles in the sample disappeared from the AUC scan after dimerization, while at the same time a new peak (that we assigned to the dimers) appeared. The small particles had a sedimentation coefficient of 35 S while the dimers had a sedimentation coefficient of 90 S. These values were converted to hydrodynamic diameter using a modified Svedberg equation and are shown at the top of Figure 3d. The AUC results confirm the Janus morphology of small NPs in solution by measuring the existence of their dimers.

We then synthesized gold NPs covered with oppositely charged ligands, MPSA and TMA. We reasoned that Janus NPs would show an electrostatic behavior that would be very different from the electrostatic behavior of the striped NPs or that of any other NPs with more homogenous distribution of ligand molecules. Janus particles would act as large dipoles, while all other distributions would have a multi-polar or more generically zwitterionic behavior. A recent theoretical paper also shows agreement with our reasoning.[28] Gel electrophoresis (GEP) is widely used in biology to separate DNA and other macromolecules, using differences in size and charge density/distribution. Thus, we argued that Janus particles could be separated from other particles due to the differences in electrostatic spatial distribution on their surface. A broadly size-distributed NP batch was used to separate the NPs using GEP. TEM showed that the NPs had a Gaussian size distribution without hint of a bi- or multimodal distribution. Yet we observed that the NPs separate into at least two distinct fractions when performing GEP: one fraction traveled with the potential, and another mostly remained still and had a long tail that moved a lot less than the initial population. (**Figure 4**) In stark contrast, homoligand NPs coated with MPSA or TMA traveled as a single population. (Figure 4a) We interpret the clear separation into two populations of the MPSA/TMA NPs as the separation between Janus and non-Janus NPs. To test this hypothesis, we extracted the two populations from the gel and characterized them by TEM to determine the size of the NPs. As shown in Figure 4b, smaller NPs are present in the first population (pop1), while larger NPs are present in the second (pop2) population. It

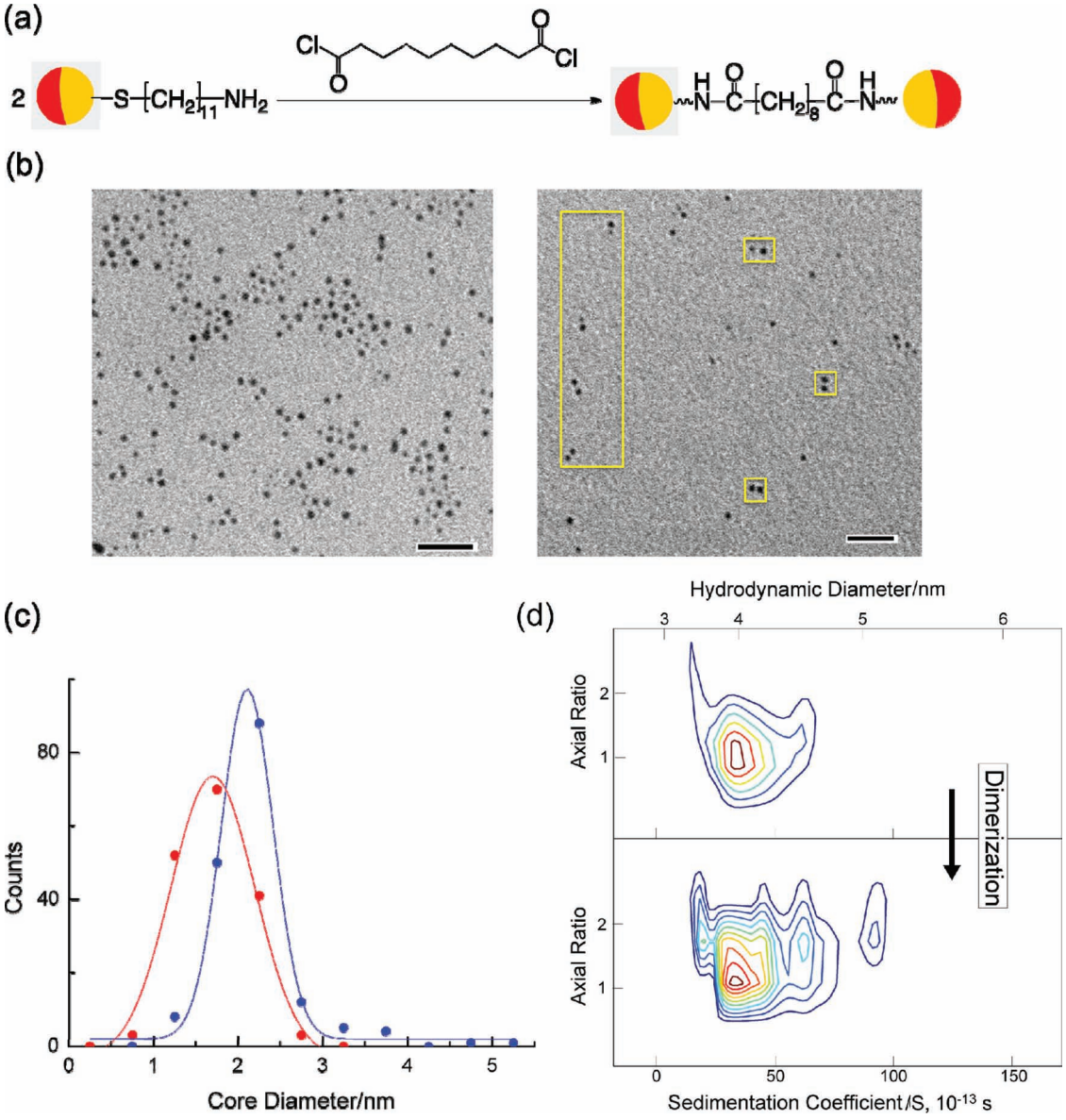

Figure 3. (a) Dimerization scheme of TDT/AUDT Janus NPs: the red and yellow indicate TDT and AUDT ligands respectively; the reaction does not need to happen in a perfect face-to-face manner, and any angle is equally probable; (b) TEM image of NPs that moved through Sephadex column (left) and that remained in the column (right). Dimers are shown in yellow box. Scale bar: 20 nm; (c) the size distribution of the particles in dimers (red) and in non-dimers (blue), indicates that only smaller sizes of NPs participate in dimerization; (d) AUC result of Janus NPs before (top) and after (bottom) dimerization: strong peak at 35 S disappears after dimerization, and new peak appears at 90 S, which shows dimers of 35 S have formed.

should be stressed that there is no gap in the size distribution of these two populations. The interpretation of our results is that pop1 is made of Janus NPs that traveled faster than striped NPs because of their dipolar nature, but they traveled slightly less than similarly sized (average size of ~1.6 nm) all-MPSA NPs that bear a larger negative charge. Pop2 contained larger non-Janus particles where both ligands roughly balance opposite charges; hence, they showed the little mobility in the gel. The average size of NPs that moved furthest (pop1) is 1.5 ± 0.5 nm, while that of NPs that moved less (pop2) is 3.8 ± 2.4 nm. Dimers and long chain-like assemblies of Janus NPs described in the literature[16a,16b] are found in the population of the smallest NPs, which also indicates that the small NPs are Janus NPs.

To further corroborate that Janus structures appear in smaller size, we used scanning tunneling microscopy (STM) to examine a sample composed of polydisperse gold NPs capped with 11-mercaptoundecanoic acid (MUA) and 1-octanethiol (OT) (1:2). The polydispersity was confirmed both by TEM (**Figure 5**a, 4.3 ± 1.0 nm) and STM (Figure 5b, 6.2 ± 1.3 nm) images. In consistent with a previous report,[29] upon the formation of two-dimensional supracrystals with these particles (in our case using Langmuir-Schaefer techniques), we observed the segregation of bigger NPs from smaller ones, both in TEM and STM

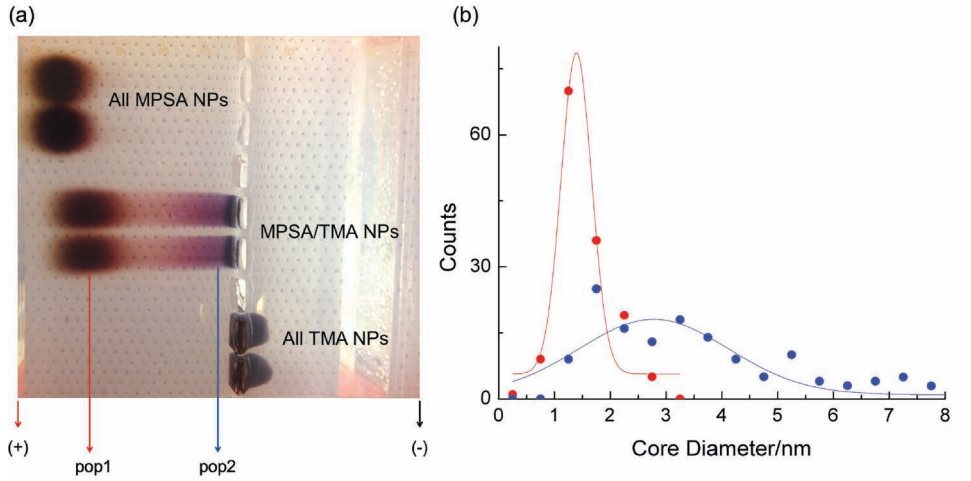

Figure 4. (a) Gel electrophoresis of TMA/MPSA Janus NPs; (b) the size distribution of NPs separated into pop1 (red), and pop2 (blue) after gel electrophoresis.

images. A close inspection of the STM image revealed the coexistence of two different ligand nanostructures, namely, striped and Janus morphology (Figure 5c, and d). Janus structure tends to appear in the small NPs, while striped structure is observed with higher frequency for larger NPs (Figure 5b).

Based on dimerization and GEP, we tried to determine the size limit of Janus NPs. Dimerization data (as shown in Figure 3c), indicate that Janus NPs exist when the core diameter is 1.5 nm or smaller and are not found for NPs larger than 3 nm. It is likely that NPs with sizes between 1.5 and 3.0 nm have either Janus or patchy morphology. These results agree well with our previous studies showing that only NPs larger than 2.0 nm have striped morphology.[3] A similar trend was observed when analyzing the results of the GEP experiments. Therefore, we can conclude that Janus NPs exist when the core diameter is smaller than 1.5 nm, and the transition between Janus-to-striped NPs observed between 1.5-3.0 nm. However, these are not absolute numbers and they will depend critically on the nature of the ligand mixture used. For example, in our STM analysis we see Janus NPs for NPs of ~5.8 nm in size. It is always difficult to determine the core size of NPs precisely by using STM images,[30] but if we use the estimation of subtracting twice the extended ligand length, we obtain that the core size of these Janus NPs is 3.1–3.2 nm. This would indicate that these NPs exist in the Janus morphology at slightly larger sizes, in agreement with our understanding that the Janus-to-striped transition will occur at larger sizes when the length mismatch between two ligands becomes smaller.[4]

In summary, we synthesized Janus gold NPs in various ligand combinations. The synthetic methods used here directly developed Janus structure without any templates

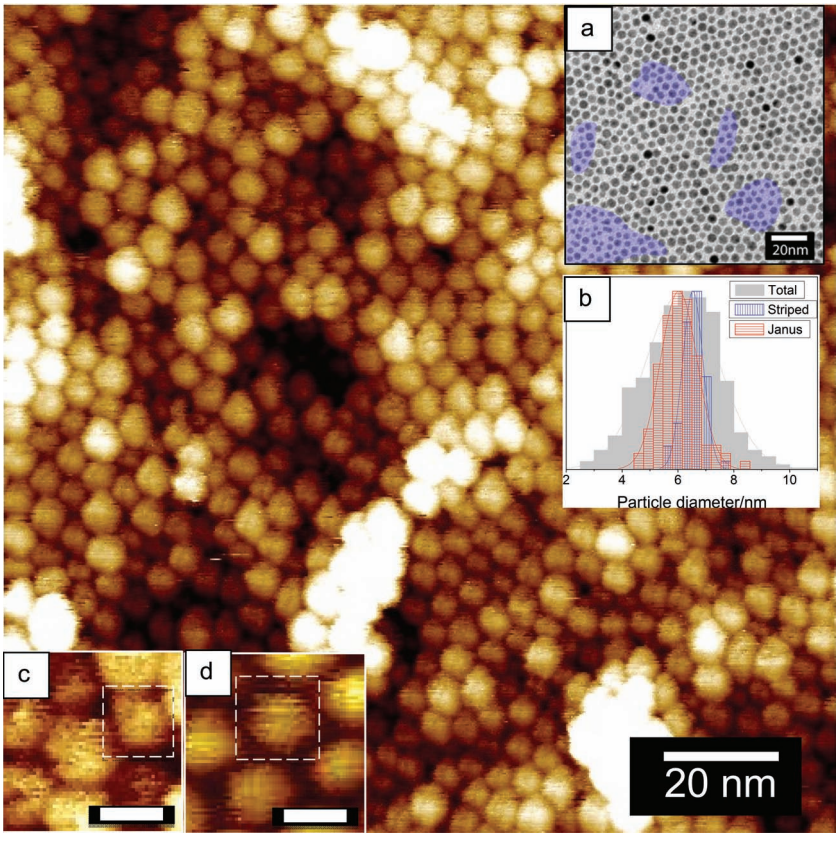

Figure 5. Monolayer of MUA:OT (1:2) gold NPs showing both Janus and striped ligand structures. Insets: (a) TEM image of the same sample where a clear separation of sizes takes places (colored blue areas represent areas with small NPs). (b) Size distribution histogram of all (grey), striped (blue) and Janus (red) NPs from STM images. (c) Close view of a Janus NP (scale bar: 5 nm). (d) Close view of a striped NP (scale bar: 5 nm).

or further modification, and the majority of NPs were Janus NPs; hence, they are available in high-yield. We also determined that gold NPs covered with two immiscible ligands form stable Janus NPs when the metal cores are smaller than 1.5 nm. Based on the size analysis, NPs larger than 3 nm would not form Janus NPs. The mixed morphologies of Janus and striped NPs are predicted to exist when the gold core size is between 1.5–3 nm.

Experimental Section

Materials: Tetradecane-1-thiol (TDT), hexadecane-1-thiol (HDT), 1-octanethiol (OT), 1,1′,4′,1″-terphenyl-4-thiol (TPT), 3-mercapto-1-propanesulfonate (MPSA), *N*,*N*,*N*-trimethyl(11-mercaptoundecyl) ammonium bromide (TMA), 11-mercaptoundecanoic acid (MUA), gold(III)chloride trihydrate ($HAuCl_4{\cdot}3H_2O$), chloro(triphenylphosphine) gold(I) ($[(C_6H_5)_3P]AuCl$), sodium borohydride ($NaBH_4$), *tert*-butylamine-borane complex morpholine borane complex, agarose, and lipophilic Sephadex were purchased from Sigma-Aldrich, and used as received. 11-Amino-1-undecanethiol hydrochloride (AUDT) was purchased from ProChimia Surfaces, and used as received. All solvents were used as received. MilliQ water (EMD Millipore) was used when water is needed. Carbon coated TEM grids were purchased from EMS Acquisition Corp. The detailed experiment for 2D NOESY NMR can be found in ref [22].

Synthesis of gold nanoparticles: Six different types of gold nanoparticles were synthesized for the experiment: (1) NPs coated with 1:1 ratio of 3-mercapto-1-propanesulfonate (MPSA) and *N*,*N*,*N*-trimethyl(11-mercaptoundecyl)ammonium bromide (TMA); (2) NPs coated with 2:1 ratio of 1-tetradecanethiol (TDT) and 11-amino-1-undecanethiol (AUDT); (3) NPs coated with 1:1 ratio of hexadecane-1-thiol (HDT) and 1,1′,4′,1″-terphenyl-4-thiol (TPT); (4) NPs coated with 1:2 ratio of 11-mercaptoundecanoic acid (MUA) and 1-octanethiol (OT); (5) NPs coated with only MPSA; (6) NPs were all-TMA NPs. Homoligand NPs, (5) and (6) were synthesized as a control sample of NPs (1).

Gold NPs covered with MPSA/TMA ligands were synthesized using one-phase method in ethanol.[24] Before adding chemicals, the solvent (ethanol) was purged in nitrogen for 30 min, and all the steps thereafter were performed in a nitrogen environment. $HAuCl_4{\cdot}3H_2O$ (177.2 mg, 0.45 mmol) was dissolved in ethanol (100 mL) at 0 °C. The 1:1 thiol mixture (MPSA, 40.1 mg, 0.225 mmol; TMA, 63.4 mg, 0.225 mmol) was added to gold solution and stirred for 10 minutes. Then, $NaBH_4$ (189.1 mg, 5 mmol) was dissolved ethanol (100 mL) and it was slowly added drop-wise using a syringe needle. Upon addition, the gold-thiol solution became turbid yellowish-green and slowly darkened to purplish-black. After the complete addition of $NaBH_4$ solution, the solution was stirred for 3 hours. Then it is placed in the refrigerator for overnight precipitation. The precipitate was filtered using vacuum filtration with quantitative filter paper, and washed with ethanol, methanol, and acetone, obtaining a shiny dark powder. Particle size distributions were measured by TEM.

As a control samples for MPSA/TMA NPs, two nanoparticle batches, one covered only with MPSA, and the other covered only with TMA are synthesized using the same one-phase method in ethanol described above. $HAuCl_4{\cdot}3H_2O$ (177.2 mg, 0.45 mmol) was dissolved in ethanol (100 mL) at 0 °C. MPSA (80.2 mg, 0.45 mmol) was added to gold solution for all-MPSA NPs, and TMA (126.8 mg, 0.45 mmol) was added to gold solution for all-TMA NPs and stirred for 10 minutes. Then, $NaBH_4$ (189.1 mg, 5 mmol) was dissolved ethanol (100 mL) and slowly added drop-wise to each of the gold solutions using a syringe needle. Particle size distributions were measured by TEM.

Gold NPs covered with HDT/TPT ligands were synthesized using a modified Stucky synthesis.[25] For small size NPs (~2.0 nm), we performed the synthesis at 0 °C, and for large size NPs (~4.5 nm), the synthesis was done at room temperature. Other reaction conditions were maintained identically for both syntheses. $[(C_6H_5)_3P]AuCl$ (123.68 mg, 0.25 mmol) was dissolved in dichloromethane (20 mL). The 1:1 mixture of thiols was added (HDT, 16.2 mg; TPT, 16.4 mg; 0.1225 mmols in total) and stirred for 10 minutes. *tert*-butylamine-borane complex (217.43 mg, 2.5 mmol) was dissolved in dicholoromethane (20 mmol), and it was added using syringe to gold-thiol mixture. The clear solution became brown and then turned darker. After addition of all of the reducing agent, the solution was stirred for 2 hours. Then, ethanol was added and the solution was placed in a refrigerator for overnight precipitation. The precipitation was filtered either using centrifuge, or vacuum filtration with quantitative filter paper and it was washed with ethanol, methanol, acetone and water. Particle size distributions were measured by TEM.

NPs coated with TDT/AUDT were synthesized using a modified Stucky synthesis. The mixture of solvents 1:2 chloroform:methanol was used. $[(C_6H_5)_3P]AuCl$ (123.68 mg, 0.25 mmol) was dissolved in the solvent mixture (10 mL). The 2:1 mixture of TDT:AUDT (TDT, 90.8 μL; AUDT, 39.75 mg; 0.5 mmol in total) was dissolved in the solvent mixture (10 mL in total) and then mixed with the gold solution and stirred for 10 min. *tert*-butylamine-borane complex (217.4 mg, 2.5 mmol) in the solvent mixture (20 mL) was added to the gold-thiol mixture. The solution was immediately put at 60 °C and left to react during one hour under strong stirring. Then the reaction was left to cool for 30 min. Part of the solvent was removed via rotary vacuum evaporation, and dimethylformamide was added to induce NPs precipitation. The solution was left to sediment for 1 day and the supernatant was subsequently removed. The rest of the purification was done with several cycles of resuspension/centrifugation in acetone. Particle size distributions were measured by TEM.

NPs coated with MUA/OT were synthesized using a similar procedure in the mixtures of solvents 1:1 toluene:methanol. $[(C_6H_5)_3P]AuCl$ (123.68 mg, 0.25 mmol) was dissolved in the solvent mixture (10 mL). The 1:2 mixture of MUA:OT (MUA, 36.4 mg; OT, 48.8 mg; 0.5 mmol in total) was dissolved in the solvent mixture (10 mL) and then mixed with the gold solution and stirred for 10 min. Borane morpholine complex (252.4 mg, 2.5 mmol) in the solvent mixture (20 mL) was added to the gold-thiol mixture. The solution was immediately put at 100 °C and left to react during one hour under strong stirring. Then the reaction was left to cool for 30 min. Acetone was added to induce NPs precipitation and the solution was left sedimenting for 1 day and the supernatant was removed. The rest of the purification was done with several cycles of resuspension/centrifugation in acetone. Particle size distributions were measured by TEM.

Dimerization of TDT/AUDT NPs: Chemical dimerization method was used for amine terminated gold NPs (TDT/AUDT NPs). We used sebacoyl chloride (SC) as the chemical linker of two particles. TDT/AUDT gold NPs (2 mg) and approximately 10-fold excess of SC (0.04 mg, 0.17 μmol) was dissolved in dichloromethane (200 μL) and allowed to react for 10 minutes. After the reaction, the mixture was cleaned using acetone and NPs were extracted. Then NPs were redissolved into dichloromethane for AUC measurement. For TEM measurement, the reacted solution was filtered through Sephadex column, separated NPs that went through the column to NPs that stayed in the column. The NPs that went through the column were extracted using acetone, and redissolved into dichloromethane. The NPs-Sephadex complex was soaked in excess amounts of dichloromethane while waiting for the Sephadex to sediment and extract NPs in the solution on the top in order to prepare the TEM sample.

TEM of gold NPs: TEM images were obtained using JEOL 200 and JEOL 2010 instrument. The TEM grids were placed on the Kim-Wipe, and 1-2 drops of the solution (~1–2 μL) were dropped on the grid and allowed it dry slowly. Self-assembled structure and dimers of Janus NPs were analyzed using ImageJ software. The structure is considered as self-assembled structure or dimers only when the inter-particle distance is less than maximum stretched length of two ligands and the linker.

Analytical ultracentrifugation: The sedimentation velocity experiments for both dimerized and non-dimerized NPs were performed using a Beckman Optical XL-A outfitted with the An-60 Ti rotor and scanning absorbance optics, in 12-mm path length double sector centerpieces with sapphire windows. The NPs were sedimented in dichloromethane at 15,000 r.p.m. at 20 °C. Data from over 50 scans were chosen to be

representative of the whole run (radial step size of 0.003 cm). The raw AUC data were analyzed with SEDFIT, an open-source computational software package available free online.

Gel Electrophoresis of charged NPs: Gel electrophoresis was performed using 3 wt% agarose gel under fixed voltage (45 V). 10% TAE buffer solution is diluted to 1% by adding milliQ water. Then, agarose (3 g) was added in 1% TAE buffer solution (100 mL). The mixture is heated using microwave for about 2 minutes until the solution becomes transparent. The solution is poured into the gel holder, removed air bubbles, and let it cool for an hour. NPs (2 mg) were dissolved in milliQ water (1 mL), and the solution (~ 40 µL) was injected to each well. The gel was placed under 45 V for 4 hours. After separation, the gel surface was cut using razor blade, and placed TEM grid inside, and voltage applied for additional 5 minutes. Then, TEM grids were dried in air covered with a laboratory dish overnight before TEM analysis.

Sample preparation (Langmuir-Schaefer Deposition) for STM imaging: Flat substrates of Au (111) on freshly cleaved mica were purchased from Phasis (Switzerland). The substrates were functionalized with 1,16-hexandecanedithiol. Langmuir-Blodgett films were prepared in a KSV 2000 with standard trough (150mm width, 78000mm^2) and symmetric barriers. NPs were dissolved in 1:1 mixture of methanol:chloroform (1mg/mL) and the solution (0.3mL) was added dropwise on the water subphase. The barriers were closed at 10 mm/min until it got to the solid-phase. Once there, the system was left to equilibrate, after which the monolayer was transferred to gold substrates in a parallel fashion (Langmuir-Schaefer deposition).

STM of MUA:OT NPs: The STM experiments were performed at room temperature using both a Veeco Multimode Scanning Probe Microscopy with E scanner in an acoustic chamber sitting on a vibration damping table in air. Mechanically cut Platinum-iridium STM tips were used. Set point currents were in the range of 30 pA to 300 pA with a voltage bias of 800-1500 mV. Integral gains varied from 0.7 to 0.5 and proportional gains from 0.5 to 0.2.

Acknowledgements

This work has been funded by a National Science Foundation CAREER Award, and a Samsung Scholarship.

Received: March 5, 2012
Published online: May 10, 2012

[1] S. J. Stranick, S. V. Atre, A. N. Parikh, M. C. Wood, D. L. Allara, N. Winograd, P. S. Weiss, *Nanotechnology* **1996**, *7*, 438.
[2] a) A. M. Jackson, Y. Hu, P. J. Silva, F. Stellacci, *J. Am. Chem. Soc.* **2006**, *128*, 11135; b) A. M. Jackson, J. W. Myerson, F. Stellacci, *Nat. Mater.* **2004**, *3*, 330.
[3] R. P. Carney, G. A. DeVries, C. Dubois, H. Kim, J. Y. Kim, C. Singh, P. K. Ghorai, J. B. Tracy, R. L. Stiles, R. W. Murray, S. C. Glotzer, F. Stellacci, *J. Am. Chem. Soc.* **2008**, *130*, 798.
[4] C. Singh, P. K. Ghorai, M. A. Horsch, A. M. Jackson, R. G. Larson, F. Stellacci, S. C. Glotzer, *Phys. Rev. Lett.* **2007**, *99*, 226106.
[5] S. C. Glotzer, M. J. Solomon, *Nat. Mater.* **2007**, *6*, 557.
[6] Z. L. Zhang, S. C. Glotzer, *Nano Lett.* **2004**, *4*, 1407.
[7] C. M. Liddell, C. J. Summers, *Adv. Mater.* **2003**, *15*, 1715.
[8] a) J. A. Champion, Y. K. Katare, S. Mitragotri, *Proc. Natl. Acad. Sci. USA* **2007**, *104*, 11901; b) R. Langer, D. A. Tirrell, *Nature* **2004**, *428*, 487.
[9] a) F. Sciortino, A. Giacometti, G. Pastore, *Phys. Chem. Chem. Phys.* **2010**, *12*, 11869; b) J. Russo, P. Tartaglia, F. Sciortino, *Soft Matter* **2010**, *6*, 4229.
[10] a) A. B. Pawar, I. Kretzschmar, *Macromol. Rapid Commun.* **2010**, *31*, 150; b) J. Z. Du, R. K. O'reilly, *Chem. Soc. Rev.* **2011**, *40*, 2402; c) H. X. Bao, W. Peukert, R. N. K. Taylor, *Adv. Mater.* **2011**, *23*, 2644.
[11] a) M. D. McConnell, M. J. Kraeutler, S. Yang, R. J. Composto, *Nano Lett.* **2010**, *10*, 603; b) S. Jiang, Q. Chen, M. Tripathy, E. Luijten, K. S. Schweizer, S. Granick, *Adv. Mater.* **2010**, *22*, 1060; c) A. Walther, A. H. E. Mueller, *Soft Matter* **2008**, *4*, 663.
[12] T. Nisisako, T. Torii, T. Takahashi, Y. Takizawa, *Adv. Mater.* **2006**, *18*, 1152.
[13] D. J. Cole-Hamilton, *Science* **2010**, *327*, 41.
[14] H. Y. Koo, D. K. Yi, S. J. Yoo, D. Y. Kim, *Adv. Mater.* **2004**, *16*, 274.
[15] N. Glaser, D. J. Adams, A. Boker, G. Krausch, *Langmuir* **2006**, *22*, 5227.
[16] a) L. Hong, A. Cacciuto, E. Luijten, S. Granick, *Nano Lett.* **2006**, *6*, 2510; b) L. Hong, A. Cacciuto, E. Luijten, S. Granick, *Langmuir* **2008**, *24*, 621; c) F. Sciortino, A. Giacometti, G. Pastore, *Phys. Rev. Lett.* **2009**, *103*, 237801; d) S. Gangwal, O. J. Cayre, O. D. Velev, *Langmuir* **2008**, *24*, 13312; e) A. Goyal, C. K. Hall, O. D. Velev, *Phys. Rev. E* **2008**, *77*, 031401.
[17] C.-H. Chen, R. K. Shah, A. R. Abate, D. A. Weitz, *Langmuir* **2009**, *25*, 4320.
[18] K. Roh, D. Martin, J. Lahann, *Nat. Mater.* **2005**, *4*, 759.
[19] Z. F. Li, D. Y. Lee, M. F. Rubner, R. E. Cohen, *Macromolecules* **2005**, *38*, 7876.
[20] a) B. Wang, B. Li, B. Zhao, C. Y. Li, *J. Am. Chem. Soc.* **2008**, *130*, 11594; b) L. Hong, S. Jiang, S. Granick, *Langmuir* **2006**, *22*, 9495; c) V. N. Paunov, O. J. Cayre, *Adv. Mater.* **2004**, *16*, 788.
[21] A. Centrone, E. Penzo, M. Sharma, J. W. Myerson, A. M. Jackson, N. Marzari, F. Stellacci, *Proc. Natl. Acad. Sci. USA* **2008**, *105*, 9886.
[22] X. Liu, M. Yu, H. Kim, F. Stellacci, unpublished.
[23] a) J. J. Kuna, K. Voitchovsky, C. Singh, H. Jiang, S. Mwenifumbo, P. K. Ghorai, M. M. Stevens, S. C. Glotzer, F. Stellacci, *Nat. Mater.* **2009**, *8*, 837; b) A. Verma, O. Uzun, Y. H. Hu, Y. Hu, H. S. Han, N. Watson, S. L. Chen, D. J. Irvine, F. Stellacci, *Nat. Mater.* **2008**, *7*, 588; c) G. A. DeVries, M. Brunnbauer, Y. Hu, A. M. Jackson, B. Long, B. T. Neltner, O. Uzun, B. H. Wunsch, F. Stellacci, *Science* **2007**, *315*, 358; d) A. Ghosh, S. Basak, B. H. Wunsch, R. Kumar, F. Stellacci, *Angew. Chem. Int. Ed.* **2011**, *50*, 7900; e) X. Liu, Y. Hu, F. Stellacci, *Small* **2011**, *7*, 1961.
[24] S. Y. Kang, K. Kim, *Langmuir* **1998**, *14*, 226.
[25] N. Zheng, J. Fan, G. D. Stucky, *J. Am. Chem. Soc.* **2006**, *128*, 6550.
[26] S. Pradhan, L. E. Brown, J. P. Konopelski, S. W. Chen, *J. Nanopart. Res.* **2009**, *11*, 1895.
[27] R. P. Carney, J. Y. Kim, H. F. Qian, R. C. Jin, H. Mehenni, F. Stellacci, O. M. Bakr, *Nat. Commun.* **2011**, *2*, 335.
[28] J. Y. Su, M. O. de la Cruz, H. X. Guo, *Phys. Rev. E* **2012**, *85*, 011504.
[29] C. J. Kiely, J. Fink, M. Brust, D. Bethell, D. J. Schiffrin, *Nature* **1998**, *396*, 444.
[30] Y. Hu, O. Uzun, C. Dubois, F. Stellacci, *J. Phys. Chem. C* **2008**, *112*, 6279.